Abundance of zinc isotopes as a marine biogeochemical tracer

Chloe N. Marechal, Emmanuel Nicolas, Chantal Douchet, Francis Albarede

Geochemistry Geophysics Geosystems G3
AN ELECTRONIC JOURNAL OF THE EARTH SCIENCES
Published by AGU and the Geochemical Society

Article
Volume 1, Number 1
26 May 2000
1015, doi:10.1029/1999GC000029
ISSN: 1525-2027

Abundance of zinc isotopes as a marine biogeochemical tracer

Chloé N. Maréchal
Laboratoire de Sciences de la Terre, UMR8515, CNRS Ecole Normale Supérieure de Lyon, F-69364, Lyon Cedex 07, France

Now at Laboratoire de Paléontologie Stratigraphique et Paléoécologie, FRE 2158, Université Claude Bernard—Lyon I, 69622 Villeurbanne Cedex, France (chloe.marechal@univ-lyon1.fr)

Emmanuel Nicolas
Laboratoire de Physique et Chimie Marines, Observatoire Océanologique de Villefranche-s/Mer, BP 28, F-06230 Villefranche sur-Mer, France

Chantal Douchet and Francis Albarède
Laboratoire de Sciences de la Terre, UMR8515, CNRS Ecole Normale Supérieure de Lyon, F-69364, Lyon Cedex 07, France (albarede@ens-lyon.fr)

[1] The Zn isotopic compositions of ferromanganese nodules, sediment trap samples, sediments, and organic reference samples have been analyzed by multiple collector inductively coupled plasma–mass spectrometry (ICP-MS). The range of isotopic variations (1‰ for $^{66}Zn/^{64}Zn$) is significant with respect to the analytical precision (0.04‰ at the 95% confidence level). Marine argillaceous sediments show rather constant values consistent with those of continental shales and loess and with the value of a basalt from Réunion Island. We infer that the depletion of the light Zn isotopes in marine particles and in ferromanganese nodules (presumably equilibrated with seawater) results from biological activity in the upper water column. The $\delta^{66}Zn$ values of sediment trap samples collected near the upwelling off the coast of Mauritania (central Atlantic) show a seasonal isotopic fluctuation consistent with biological pumping during the high-productivity period. Higher values of $\delta^{66}Zn$ in nodules appear to be associated with the amplitude of seasonal variations rather than with the mean values of the biological productivity.

Components: 7082 words, 10 figures, 5 tables.

Keywords: zinc; zinc isotopes; nutrients; sedimentation.

Index Terms: 4870 Oceanography: Biological and Chemical: Stable isotopes (0454, 1041); 1065 Geochemistry: Major and trace element geochemistry; 4267 Paleoceanography.

Received 31 October 1999; **Revised** 5 March 2000; **Accepted** 9 March 2000; **Published** 26 May 2000.

Maréchal, C. N., E. Nicolas, C. Douchet, and F. Albarède (2000), Abundance of zinc isotopes as a marine biogeochemical tracer, *Geochem. Geophys. Geosyst.*, *1*, 1015, doi:10.1029/1999GC000029.

1. Introduction

[2] As other biolimiting elements, Zn is depleted by the biological pump from the surface water and is regenerated in the deeper waters through oxidation of organic matter by bacterial activity [*Bruland*, 1980; *Bruland and Franks*, 1983; *Bruland et al.*, 1994; *Saager*, 1994]. It is believed

that in high-nutrient, low-chlorophyll areas, a few of these elements may limit the marine biological productivity [*Martin and Fitzwater*, 1988; *Morel et al*., 1991]. The geochemical cycle of these elements in the superficial envelopes therefore influences the marine biological productivity and, in turn, the global environment by shifting the atmospheric CO_2 pumped during photosynthesis. The comprehension of the mechanisms which sustain the past and present oceanic cycles of these trace metals is therefore of major importance. Although Zn and Cd are chemically broadly similar (they both belong to the group IIB of the periodic table), their behavior in the water column is different: Cd is rapidly regenerated, just as P is, whereas Zn is largely exported, just as Si is. Given the wealth of information conveyed by Cd as an indicator of primary productivity in ancient oceans [*Boyle and Keigwin*, 1985/1986], we therefore anticipate that Zn and its isotopes may carry a signal of paleoceanographic importance.

[3] Because of a small relative mass difference, the chances of observing a significant isotopic fractionation for Zn isotopes critically depend on the precision of the measurement. So far, conventional analysis of Zn isotopes by thermal ionization mass spectrometry (TIMS) using a double-spike procedure produces data with an inadequate precision, in the order of several per mil [*Rosman*, 1972]. The measurements by TIMS directed at identifying Zn isotopic heterogeneities in meteorites [*Loss and Lugmair*, 1989, 1990; *Gawinowski et al*., 1989; *Völkening and Papanastassiou*, 1990] should be disregarded, as they involve a step of internal normalization to a reference isotopic ratio which destroys all information about mass-dependent fractionation and therefore about any natural terrestrial variations. Multiple collector plasma source mass spectrometer (essentially a standard mass spectrometer equipped with a double-focusing magnetic sector and an array of Faraday cups and fitted with a plasma source) now makes the high-precision isotopic measurements possible. This recent substantial improvement in mass spectrometric techniques has elicited the present work on Zn isotopes in marine material and sediments.

[4] The motivation of the present work is to estimate the potential of Zn isotopes as oceanographic tracers: Is an isotopic signal present at all and, if present, does it trace the strength of local biological productivity or, just as the elemental concentration of these nutrient-like elements, does it change with the aging of the water masses? Zn enters biochemical cycles largely as enzymatic components and mediate extremely fast biological reactions: For example, Zn is used for the conversion of CO_2 to HCO_3^- by carbonic anhydrase in the photosynthesis process. Zn is also used for the regulation of gene expression [*Lippard and Berg*, 1994; *Frausto da Silva and Williams*, 1991]. In addition, ferromanganese crusts and nodules may contain up to a few thousand ppm Zn, which signals that this element is efficiently adsorbed by particles with a large surface area. Because biological activity preferentially affects the chemical bonds of the lighter isotopes, some Zn isotopic fractionation may therefore be anticipated between the dissolved Zn and particulate (biogenic and detrital) phases. The determination of the isotopic compositions of dissolved Zn, especially from surface water (<100 p*M*/kg in pelagic areas to 300 p*M*/kg in upwelling coastal regions [*Bruland and Franks*, 1983]), would require the extraction of this element from very large volume samples. We therefore measured the isotopic composition of Zn in material extracted from the outer layer of ferromanganese nodules so that the isotopic variability of this element with water depth and geographic situation in a phase that could mirror seawater properties can be established for the first time. We also determined the Zn isotopic composition in marine particles sampled in the equatorial Atlantic over a 1-year interval in order to assess whether the variations with time and depth are consistent with the picture that emerges from the nodule isotopic map. Finally, the possibility that diagenetic fluids affect the marine Zn cycle and the preservation of Zn isotopic compositions down the sedimentary column was also indirectly evaluated by measurements in pelagic sediments from various depths and different oceanic areas.

2. Sampling

[5] We analyzed the Zn isotopic compositions of the surface layers from 40 nodules from the Atlantic, Indian, and Pacific Oceans and the circum-Antarctic region. The geographic location of the samples is shown in Figure 1. The samples were obtained from various collections and core repositories around the world. Most of them were previously analyzed for Nd and Hf isotopes by *Albarède et al*. [1997, 1998] and for Pb isotopes by *Abouchami and Goldstein* [1995] and *Abouchami et al*. [1999].

[6] The sediment traps were moored at 250, 1000, and 2500 m in the upwelling off the coast of Mauritania (central Atlantic Ocean) under meso-

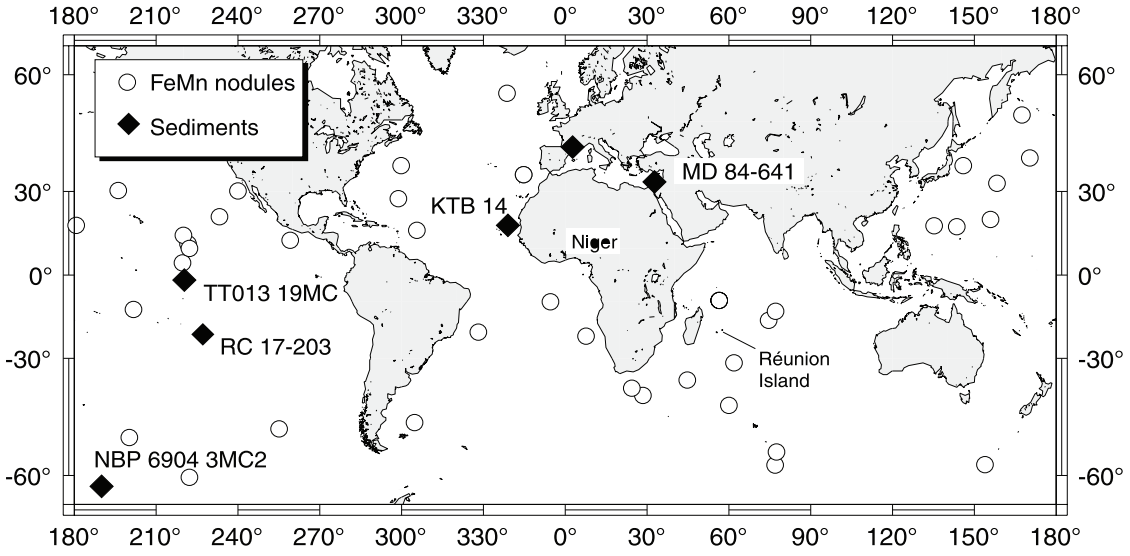

Figure 1. Map of sample localities.

trophic conditions in an area where the integrated primary production is ~125 g C m^{-2} yr^{-1} [*Auffret et al.*, 1992]. The site is located at 18°30′N, 21°06′W, some 400 km from the coast and with a water depth of 3100 m [*Legeleux et al.*, 1994]. It is part of the French Joint Global Flux Study (JGOFS) Eutrophic, Mesotropic, and Oligotrophic Sites (EUMELI) survey program [*Morel*, 1996]. Before deployment, the traps were sterilized with formaldehyde. The present data correspond to samples taken between February 1991 and January 1992, mostly at intervals of 10 days. A substantial fraction of the samples collected at 250 m were not processed because of high current velocities and stronger lateral transport. The particles collected are composed of carbonates (50–80%), clay and other lithogenic matter (15–35%), organic matter (10–20%), and biogenic opal (<10%) [*Wefer and Fischer*, 1993; A. Bory et al., manuscript in preparation, 2000]. Particle fluxes show two maxima which correspond to a spring bloom and a summer bloom, about 60 and 50 days long, respectively [*Leblond et al.*, 1995]. The particle sinking rate during the blooms was estimated to be ~500 m d^{-1} [*Bory*, 1997].

[7] Sediment samples were collected at the EUMELI site and in the central and South Pacific Ocean (Figure 1). Sediment core KTB 14 (18°28′N, 21°03′W) was sampled with a multiple corer at the EUMELI mesotrophic site in May–June 1992 [*Legeleux et al.*, 1994]. The core was sliced in 0.5- to 1.0-cm intervals, dried at 110°C, and ground in an agate mortar. The surface sediment is essentially composed of marl ooze with nanofossils. Carbonates account for 62% of the particle content from the surface to 5 cm depth [*Auffret et al.*, 1992]. The sedimentation rate at this site has been estimated to 15 mm kyr^{-1}. Fifteen samples have been analyzed from the surface to 23 cm depth, which corresponds to the deglaciation period from the Last Glacial Maximum (circa 15,000 years B.P.). The samples taken at shallower depth correspond to the Holocene. A depth profile was obtained on the core sediment RC 17-203 from the tropical Pacific Ocean (21°50′S, 132°53′W) at depths from 3 to 160 cm. The sediment is composed of red clay. The surface sample NBP6904 3MC2 (61°57′S, 170°03′W) contains ~10% carbonates and 75% biogenic opal, while TT013 19MC (01°52′S, 139°43′W) is composed of 80% carbonates and 5–10% opal. These Pacific sediments were sampled with a multicorer (R. A. Anderson, personal communication, 2000). We also determined the isotopic compositions of a glacial (S6) and two interglacial (S1 and S5) sapropels collected in the Mediterranean (33°02°N, 32°38′E) and of two shales and a black shale from the Paleozoic Montagne Noire of France. Finally, an eolian dust (A19) scraped from the wing of a domestic plane in Niger was analyzed as a reference for lithogenic inputs.

[8] We have also analyzed three organic reference samples, the lobster liver CRM TORT-2 from Prince Edward Island (North Atlantic), the mussel tissue CRM 278 from the Waddenzee (Netherlands), and the plankton CRM 414 from a pond next to the Po River (Italy), plus a sample of

Table 1. Zn Isotope Compositions of Nodules[a]

Sample	δ^{66}Zn, ‰	Zn,[b] ppm	Co,[a] ‰	Depth, m	Latitude	Longitude
			Atlantic Ocean			
RC15–D19	0.72			5792	27°36′N	61°08′W
RC11–6PC	0.63			5707	16°38′N	54°21′W
RC13–D5	0.85			1394	09°58′S	05°23′W
RC15–D5	1.02			2655	48°28′S	55°14′W
RC15–D13	0.53			4146	20°58′S	31°48′W
V19–D11	0.78			4600	38°04′N	60°13′W
V27–D5	1.03			1575	56°16′N	21°24′W
V29–D12	1.00			3265	22°27′S	07°33′E
65 GTV	0.90			1500	35°20′N	15°20′W
65 GTV (duplicate)	0.69					
			Indian Ocean			
V34–D25	0.89			4650	39°07′S	24°22′E
V34–D26	0.83			4105	41°16′S	28°24′E
RC14–D3	0.92			2265	36°45′S	44°46′E
MV74–2 SBT	0.77			4500	04°32′N	140°21′W
CP8130	0.79	1425	0.108	5270	13°35′S	77°03′E
DR7506	0.95	804	0.149	4840	44°00′S	59°57′E
DR7301	0.97	640	1.215	2660	09°36′S	56°24′E
AET7610	0.97	603	0.197	4245	31°21′S	61°55′E
AET7718	0.85	698	0.214	4430	16°49′S	74°38′E
			Pacific Ocean			
V18–SBT120	0.82			5000	12°52′S	158°19′W
RC11–D19	0.70			5000	14°52′N	140°02′W
RPOC–76 (SBT–5)	0.79			5000	11°44′N	138°21′W
ANT 24	0.91			4700	18°18′N	135°15′E
ANT 23	1.01			2500	32°43′N	158°16′E
ZETES 9	0.80			4500	38°01′N	145°59′E
ZETES 11	1.06			1500	40°16′N	170°19′E
TUNES 65	1.03			3000	20°27′N	155°55′E
RNDB 60	0.98			2500	51°31′N	167°32′E
MERO 2P52	0.95			5000	09°57′N	137°47′W
CERS–10D	0.84			3500	12°59′N	100°53′W
MARA–11	0.81			5000	17°51′N	143°30′E
RNDB 10–68D	0.67			4000	18°27′N	179°17′W
DWBD–1	0.98			4500	21°27′N	126°43′W
WSFL 2D LEGO	1.05			2500	30°12′N	120°03′W
ARES 57D	1.01			3000	30°21′N	163°51′W
			Circum–Antarctic Current			
E14–12 RD146	1.02			2853	52°01′S	159°53′W
E25–12 BT237	1.00			3877	49°59′S	104°53′W
E20–13 BT205	0.99	890	0.051	4289	60°20′S	137°46′W
E27–40 BT27–28	1.01	1150	0.180	3542	57°55′S	153°57′E
DR8605	1.16	716	1.055	2600	58°02′S	77°01′E
DR8607	1.12	618	0.544	2510	55°18′S	77°28′E

[a] Delta values are calculated with respect to the standard solution JMC 3–0749 L. Analytical error is 0.04‰.
[b] *Albarède et al.* [1997].

copepode-rich zooplankton from the Ligurian Sea (Mediterranean) collected in May 1995. For reference, we also analyzed Zn extracted from a sample of human blood.

[9] Finally, a modern basalt from the Piton de la Fournaise volcano (Réunion Island, Indian Ocean, RUE 928 27) was analyzed as a reference for mantle-derived material.

3. Analytical Procedure

[10] For ferromanganese nodules, 2–4 mg of sample were dissolved in 0.5 mL of concentrated aqua

Table 2. Zn Isotopic Compositions of Igneous and Sedimentary Material[a]

Sample	Age	δ^{66}Zn, ‰	Depth, cm	Water Depth, m	Latitude	Longitude
		Basalt (Piton de la Fournaise, Réunion Island)				
RUE 928–27	0.25					
		Shales (Montagne Noire of France)				
J5	Visean	0.27				
IZN4 (black shale)	Devonian	0.32				
BDX2	Tremadoc	0.20				
		Eolian Dust (Niger)				
A19	0.17					
		Sapropel (Mediterranean)				
MD 84 641 – S1	Holocene	0.26	33	1375	33°02′N	32°38′E
MD 84 641 – S5	125 kyr	0.29	378		33°02′N	32°38′E
MD 84 641 – S6	175 kyr	0.29	469		33°02′N	32°38′E
		Deep–Sea Surface Sediments				
KTB 14		0.22	0.0–0.5	3100	18°28′N	21°03′W
(15 mm/kyr^{-1})		0.25	0.5–1.0			
		0.22	1.0–1.5			
		0.20	1.5–2.0			
		0.21	2.0–2.5			
		0.25	2.5–3.0			
		0.27	5.0–5.5			
		0.20	5.5–6.0			
		0.21	6.0–6.5			
		0.22	6.5–7.0			
		0.26	7.0–8.0			
		0.18	8.0–9.0			
		0.22	9.0–10.0			
		0.19	13.0–14.0			
		0.25	22.0–23.0			
RC 17–203		0.24	3–30	3900	21°50′S	132°53′W
		0.23	14–16			
		0.30	20–22			
		0.35	116			
		0.17	160			
NBP 6904 3MC2		0.69	3.0–4.0	3404	61°57′S	170°03′W
TT013 19MC		0.79	1.0–2.0	4500	01°52′S	139°43′W

[a] Delta values are calculated with respect to the standard solution JMC 3–0749 L. Analytical error is 0.04‰. KTB 14 corresponds to a sediment cored at the mesotrophic site of EUMELI (central Atlantic Ocean).

regia and evaporated to dryness, and the procedure was repeated. The sediment trap samples were first rinsed in deionized water on a cellulose membrane to remove sea salt and were then dehydrated. The sedimentary material (inclusive of the filter for trap material) was dissolved in 0.5 mL HNO_3, evaporated to dryness, and then dissolved in a HF + HNO_3 mixture. Upon treatment of the nodules or sedimentary samples through these initial steps, the evaporated residue was then taken up in concentrated HCl. It was found that adding $HClO_4$ makes no difference, which suggests that Zn is not involved in fluoride precipitation.

[11] The chemical purification of Zn sample and the mass spectrometry procedure are described in detail by *Maréchal et al.* [1999]. The samples were processed in a clean room with filtered air and under laminar-flow hoods. Suprapur Merck reagents together with acids distilled in Vycor stills or in a Teflon two-bottle setup were used. Samples were dissolved in Savillex^{TM} perfluoroalkoxy (PFA) capsules. Zn was isolated by anion exchange chemistry on Biorad macroporous resin AG MP-1. The total Zn blank (15–50 ng) represents typically <2–3 percent of the samples. The isotopic abundances were measured in Lyon by plasma source mass spectrometry. The instrument, called the Plasma 54, is equipped with a magnetic sector and multiple collection. The $^{66}Zn/^{64}Zn$ isotopic ratios were corrected from instrumental mass frac-

Table 3. Zn Isotopic Composition of Biological Material[a]

Sample	δ^{66}Zn, ‰
Lobster liver (CRM TORT-2)	0.51
Mussel tissue (CRM 278)	0.82
Plankton (CRM 414)	0.42
Zooplankton	0.16
Human blood	0.41

[a] The sample of zooplankton was collected in the Mediterranean sea in May 1995 (EIMETO – DYFAMED cruise). Analytical error is ±0.04%.

tionation with respect to the isotopic composition of a Cu National Institute of Standards and Technology (NIST) Standard Reference Material (no. 976) added to the purified Zn sample and further recalibrated by running a Zn isotopic standard solution in alternance. The isotopic data are expressed as a deviation of the sample $^{66}Zn/^{64}Zn$ from the value obtained for the JMC 3-0749 L standard in delta (per mil) notation:

$$\delta^{66}Zn_{JMC} = \left[\frac{(^{66}Zn/^{64}Zn)_{sample}}{(^{66}Zn/^{64}Zn)_{JMC}} - 1\right] \times 10^3 \qquad (1)$$

[12] The overall external precision achieved by the analytical technique is conservatively estimated at 0.04‰ at 2-σ level. The remarkable uniformity of δ^{66}Zn values of ferromanganese nodules from the Circum-Antarctic Current in the Pacific sector and down the core for KTB 14 (Tables 1 and 2) as well as the consistency of results for successive analyses of EUMELI sediment traps confirm that this estimate is reasonable.

[13] The δ^{66}Zn values of the organic reference materials vary from 0.42 to 0.82‰ (Table 3) but with the Zn of the Mediterranean copepodes being significantly lighter (0.16‰).

4. Results

[14] The isotopic compositions of Zn in ferromanganese nodules are listed in Table 1 and shown on the map of Figure 2. The δ^{66}Zn values range from 0.53 to 1.16‰, with a mean value of 0.90 ± 0.28‰ at 95% confidence level (41 values). The range of variation therefore corresponds to 16 times to the analytical precision. The values seem to be regularly distributed amongst the different oceanic areas: values of ~0.6–0.8‰ dominate in the central Pacific and central Atlantic, whereas they are mostly larger than 1.0 in the Southern Ocean, the North Pacific, and the North Atlantic. Zn therefore seems to be predominantly lighter in the intertropical zones, especially in the Northern

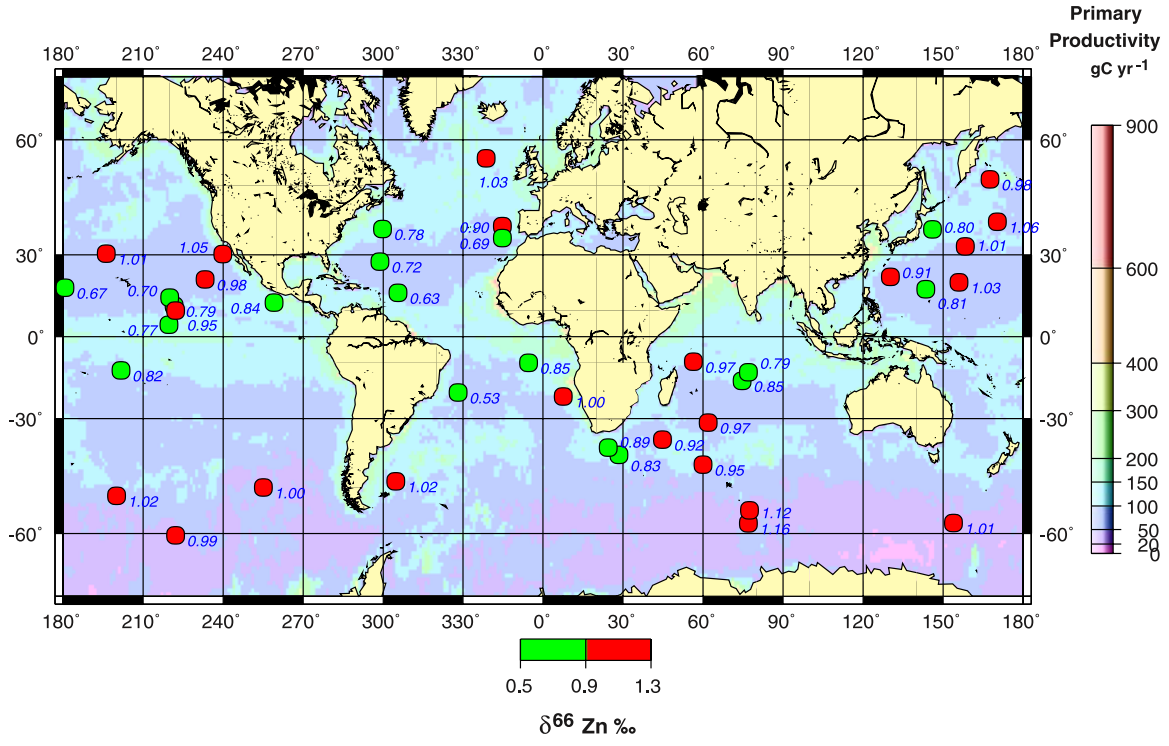

Figure 2. Distribution of δ^{66}Zn (‰) values in ferromanganese nodules with respect to the distribution of biological primary productivity. Productivity data are from *Antoine et al.* [1996].

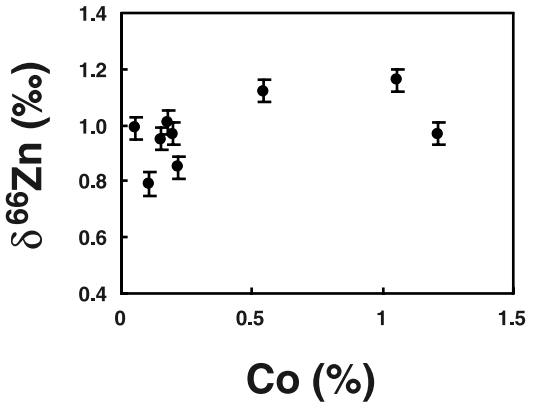

Figure 3. Distribution of δ^{66}Zn versus Co concentrations measured in nodules. The error bars correspond to ±0.04‰.

Hemisphere, and heavier in the polar regions. Higher δ^{66}Zn values are also observed off the Namibian coast and in the northwestern part of the Indian Ocean. Two aliquots from a same encrustation sampled in the tropical Atlantic next to the Mediterranean outflow differ by almost 0.3‰, in agreement with the large isotopic Nd and Pb isotopic heterogeneities reported from this particular encrustation by *Abouchami et al*. [1999].

[15] The Zn isotopic properties do not visibly vary with Zn concentrations (Table 1), which may simply reflect that the samples are too few for such a correlation to be meaningful. They seem not to vary significantly with the Co concentration either

Table 4. Zn Isotopic Compositions of Marine Particles Collected at 250, 1000, and 2500 m Depth at the Mesotrophic Site of EUMELI (18°30′N, 21°06′W, Central Atlantic Ocean)[a]

		250 m		1000 m		2500 m	
Period	Days	Sample	δ^{66}Zn, ‰	Sample	δ^{66}Zn, ‰	Sample	δ^{66}Zn, ‰
Feb. 1–13, 1991	1	II 4 M 1	0.27	II 3 M 1	–	II 2 M 1	0.18
Feb. 13–23, 1991	10	II 4 M 2	0.35	II 3 M 2	0.25	II 2 M 2	0.24
Feb. 23 to March 5, 1991	10	II 4 M 3	0.38	II 3 M 3	0.28	II 2 M 3	0.24
March 3–15, 1991	10	II 4 M 4	0.29	II 3 M 4	0.26	II 2 M 4	0.19
March 15–25, 1991	10	II 4 M 5	0.38	II 3 M 5	–	II 2 M 5	0.28
March 25 to April 4, 1991	10	II 4 M 6	–	II 3 M 6	–	II 2 M 6	0.33
April 4–14, 1991	10	II 4 M 7	0.35	II 3 M 7	0.32	II 2 M 7	0.31
April 14–24, 1991	10	II 4 M 8	0.43	II 3 M 8	0.29	II 2 M 8	0.31
April 24 to May 4, 1991	10	II 4 M 9	0.34	II 3 M 9	0.36	II 2 M 9	0.33
May 4–14, 1991	10	II 4 M 10	0.43	II 3 M 10	0.28	II 2 M 10	0.31
May 14–24, 1991	10	II 4 M 11	–	II 3 M 11	0.27	II 2 M 11	–
May 24 to June 3, 1991	10	II 4 M 12	–	II 3 M 12	0.35	II 2 M 12	0.28
June 3–13, 1991	10	II 4 M 13	0.35	II 3 M 13	0.32	II 2 M 13	–
June 13–23, 1991	10	II 4 M 14	0.28	II 3 M 14	0.33	II 2 M 14	0.28
June 23 to July 3, 1991	10	II 4 M 15	0.29	II 3 M 15	0.33	II 2 M 15	0.31
July 3–13, 1991	10			II 3 M 16	0.36	II 2 M 16	–
July 13–23, 1991	10			II 3 M 17	0.28	II 2 M 17	0.32
July 23 to Aug. 2, 1991	10			II 3 M 18	–	II 2 M 18	–
Aug. 2–12, 1991	10			II 3 M 19	0.36	II 2 M 19	0.26
Aug. 12–22, 1991	10			II 3 M 20	0.16	II 2 M 20	0.21
Aug. 22 to Sept. 1, 1991	10			II 3 M 21	–	II 2 M 21	0.28
Sept. 1–11, 1991	10			II 3 M 22	0.22	II 2 M 22	0.24
Sept. 11–12, 1991	1			II 3 M 23	–	II 2 M 23	0.22
Sept. 12–13, 1991	1			II 3 M 24	–	II 2 M 24	0.21
Sept. 13–19, 1991	6						
Sept. 19–29, 1991	10					III 2 M 1	0.18
Sept. 29 to Oct. 9, 1991	10					III 2 M 2	0.16
Oct. 9–19, 1991	10					III 2 M 3	0.19
Oct. 19–29, 1991	10					III 2 M 4	0.16
Oct. 29 to Nov. 8, 1991	10					III 2 M 5	0.22
Nov. 8–18, 1991	10					III 2 M 6	0.23
Nov. 18–28, 1991	10					III 2 M 7	0.15
Nov. 28 to Dec. 8, 1991	10					III 2 M 8	0.23
Dec. 8–18, 1991	10					III 2 M 9	0.22
Dec. 18–28, 1991	10					III 2 M 10	0.22
Dec. 28, 1991, to Jan. 7, 1992	10					III 2 M 11	0.21
Jan. 7–17, 1992	10					III 2 M 12	0.24

[a] The hiatus at 250 and 1000 m is due to high current velocities and strong lateral transport.

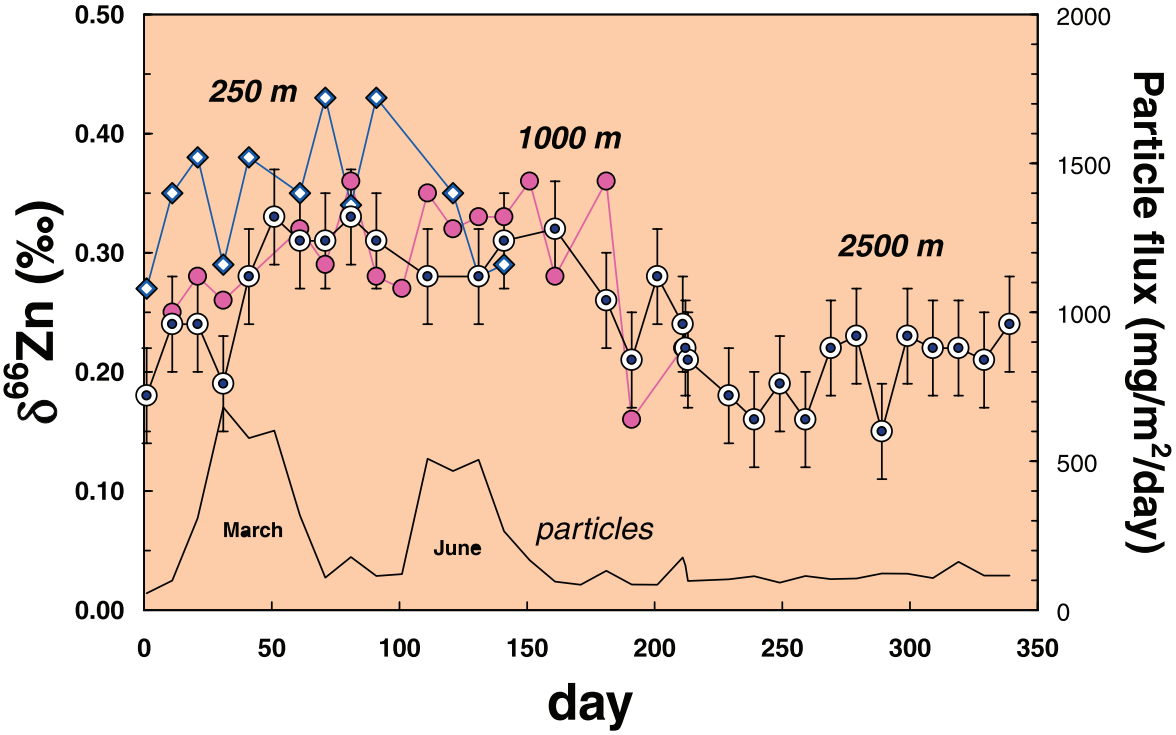

Figure 4. The δ^{66}Zn in marine particles trapped at 250, 1000, and 2500 m depth at the mesotrophic site of EUMELI (central Atlantic Ocean) from February 1991 to January 1992. The normal sampling interval is 10 days. Particle fluxes at 2500 m depth (A. Bory et al., manuscript in preparation, 2000) are also shown. The error bars correspond to ±0.04‰.

(Figure 3) and therefore are independent of the growth rate [*Halbach et al.*, 1983].

[16] The δ^{66}Zn values of particulate matter at EUMELI are listed in Table 4 and are presented as a function of depth in Figure 4 along with the particle flux (A. Bory et al., manuscript in preparation, 2000). The variability decreases consistently with depth. The values of δ^{66}Zn also decrease with depth, with a maximum value of 0.43‰ in the upper trap and a minimum value of 0.15‰ in the lower trap. During the blooms the delta values decrease progressively from the upper trap to the lower trap (Table 5 and Figure 5). This is corroborated by data obtained both from the same site at a later period and from a different, oligotrophic, site from the EUMELI project [*Maréchal*, 1998]. A similar variation of δ^{66}Zn in the water column is observed for the ferromanganese nodules (Figure 6).

[17] Despite some residual noise, the δ^{66}Zn record of the sediment trap material appears to vary smoothly with time. At 2500 m the isotopic rollover is particularly regular and the range exceeds the analytical uncertainty. The rollover can be broken down into two humps, barely distinguishable within the analytical precision. These two humps are shifted by a few weeks with respect to each bloom event, a delay presumably equivalent to the mixing time of Zn in the surface layer.

[18] The δ^{66}Zn values of sediments are presented in Table 2. The samples from EUMELI and the tropical Pacific (RC 17-203) show no sign of variation with depth (Figure 7). The mean of 20 δ^{66}Zn values is 0.23 ± 0.08‰ (2-σ), which is consistent with the values of the sapropels (0.28 ± 0.02‰), of the shales (0.20–0.32‰) and with the value of 0.17‰ obtained on the sample of eolian dust from Niger. The δ^{66}Zn values of the interglacial (S1 and S5) and glacial (S6) sapropels are indistinguishable. It is only slightly lighter than the 0.30–0.38‰ range of European loess data (J. M. Luck and D. Ben Othman, personal communication, 1999). It is also comparable with the average δ^{66}Zn value of 0.17 ± 0.38‰ obtained on 17 sphalerite samples [*Maréchal*, 1998] and on the Réunion Island basalt (0.25‰). The δ^{66}Zn of the other two sediments from the Pacific are significantly higher, 0.69‰ for NBP6904 3MC2 and 0.79‰ for TT013 19MC. The isotopic composition of the sediments therefore seems to be a function of their composi-

Table 5. Average Particulate Zn Concentrations and Isotopic Compositions of Particulate Samples Taken at the Mesotrophic and Oligotrophic Sites of EUMELI[a]

Samples	Trap Depth, m	δ^{66}Zn, ‰	Zn, μg/g
Spring Bloom, March 1991 (2 Samples), EUMELI Mesotrophic Site			
II 4 M (average 3–4)	250	0.34	61
II 3 M (average 3–4)	1000	0.27	46
II 2 M (average 3–4)	2500	0.22	22
Summer Bloom, June 1991 (2 Samples), EUMELI Mesotrophic Site			
II 3 M (average 12, 14)	1000	0.34	39
II 2 M (average 12, 14)	2500	0.28	22
July to Dec. 1992 (15 Samples), EUMELI Mesotrophic Site[b]			
IV 3 M (average 5–24)	1000	0.24	88
IV 2 M (average 5–24)	2500	0.19	53
April to Sept. 1991 (11 Samples), EUMELI Oligotrophic Site[b]			
II 3 O (average 7–22)	1000	0.23	90
II 2 O (average 7–22)	2500	0.19	55

[a] The concentrations were measured at Villefranche-sur-Mer by voltamperometric adsorption. The samples II *i* M 3, II *i* M 4, and II *i* M 12, II M *i* 14 for *i* = 2, 3, 4 correspond to the peaks of the spring and summer blooms, respectively, at the mesotrophic site (see Table 4). The flux of particles remains constant with depth during the period corresponding to the samples referred to in this table. For an observed settling velocity of 500 m d^{-1}, the Zn concentrations and isotopic compositions therefore characterize a same sedimentation event collected at different depths.
[b] *Maréchal* [1998].

tion: the higher their abundance in carbonate and silica, the higher their δ^{66}Zn.

[19] The whole data are summarized in Figure 8. The δ^{66}Zn values spread over 1‰, which is large compared to the analytical error of 0.04‰. It generally appears that nodules have higher values (~0.9‰) than sediment traps and sediments samples (0.2–0.3‰).

5. Discussion

[20] The present data suggest that the source of Zn isotope variability is associated with biological productivity and the remineralization of organic material in the water column. In this respect, δ^{66}Zn is a tracer similar to δ^{13}C and δ^{15}N. The lighter isotope ^{64}Zn is preferentially removed from surface waters, which is a constant property of biological activity in all isotopic systems. A negative correlation between δ^{66}Zn and depth is indeed visible in the EUMELI sediment traps (Table 5 and Figure 5) and, to a different extent, in ferromanganese nodules (Figure 6). At EUMELI, the isotopic effect parallels the decrease of Zn concentrations in the particles (Figure 5). Likewise, the δ^{66}Zn of the sediment trap material increases during the spring and subsequently declines in late summer. Smaller humps follow the blooms after a lag of a few weeks (Figure 4).

[21] The preferential incorporation of the light isotope into biological material observed in the particulate material cannot, at this stage, be assigned to specific mechanisms of Zn transfer between seawater and the particles. The consistent decrease of Zn concentrations and isotopic compositions with depth in sediment traps suggests that remineralization [*Jickells et al.*, 1996] plays a major role with respect to isotopic variability (Figure 5). In the absence of isotopic data on dissolved Zn, it is premature to argue about whether isotopic fractionation between biogenic particles and seawater takes place at equilibrium or in purely kinetic conditions.

[22] The source effects on both the geographic patterns of nodules and EUMELI isotopic time series, notably at 2500 m, are almost certainly negligible because all the samples derived from the continental crust and the mantle fall within a relatively narrow range of δ^{66}Zn around 0.30‰. In addition, the residence time of Zn in the deep ocean is too long (3000–6000 years according to *Bruland et al.* [1994]) for input fluctuations over a very short period of time to affect the oceanic Zn inventory. This is confirmed by the lack of significant Zn isotopic fluctuations in the sedimentary column at the EUMELI site. Moreover, the relative homogeneity of δ^{66}Zn values in the sedimentary column from the EUMELI site and from the tropical Pacific (RC 17-203) indicates that diage-

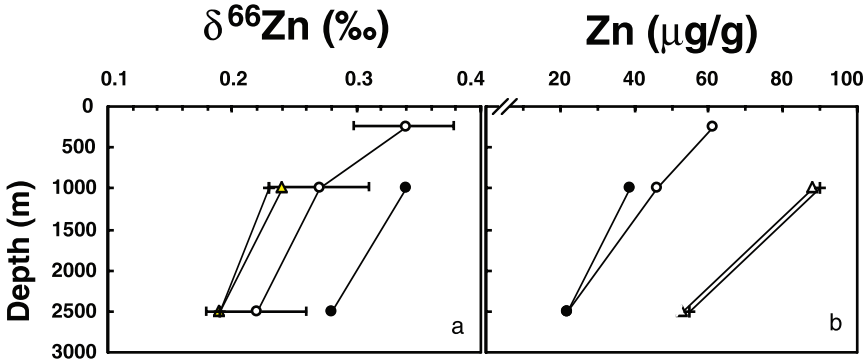

Figure 5. Mean (a) δ^{66}Zn and (b) Zn concentration of the particles collected at different depths at the EUMELI sites (central Atlantic) (see Table 5). Pluses, oligotrophic site. Other symbols refer to the mesotrophic site: open circles, spring bloom 1991; closed circles, summer bloom 1991; triangles, July to December 1992. The error bars correspond to ±0.04‰.

netic fluids do not act as a strong source of isotopically fractionated Zn for the water column and do not seem to obliterate the Zn isotopic signature of the sediments.

[23] The sediments with the lowest content in carbonates and silica (RC 17-203 and KTB 14) have δ^{66}Zn values indistinguishable from those of terrigenous material, such as shales, eolian particles, loess, or sphalerite (0.2–0.4‰). The Zn from Mediterranean sapropels that was expected to show a strong biological signal also seems to be dominated by a lithogenic signal. In contrast, Zn in the two samples dominated by either silica (NBP6904 3MC2) or carbonates (TT013 19MC) is isotopically heavier and falls in the lower part of the ferromanganese nodule range (Figure 8). This indicates that Zn from these samples is probably dominated by oxihydroxide coatings or micronodules associated with carbonates or silica.

[24] Because ferromanganese nodules grow very slowly, typically at a rate of millimeters per thousand years, the significance of their geochemical

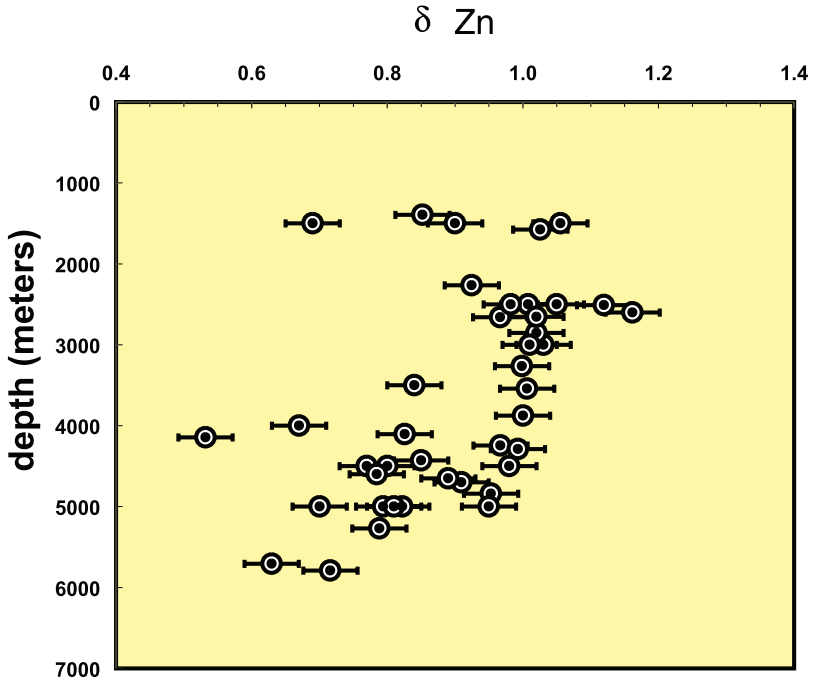

Figure 6. Distribution of δ^{66}Zn in nodules as a function of depth. The error bars correspond to ±0.04‰.

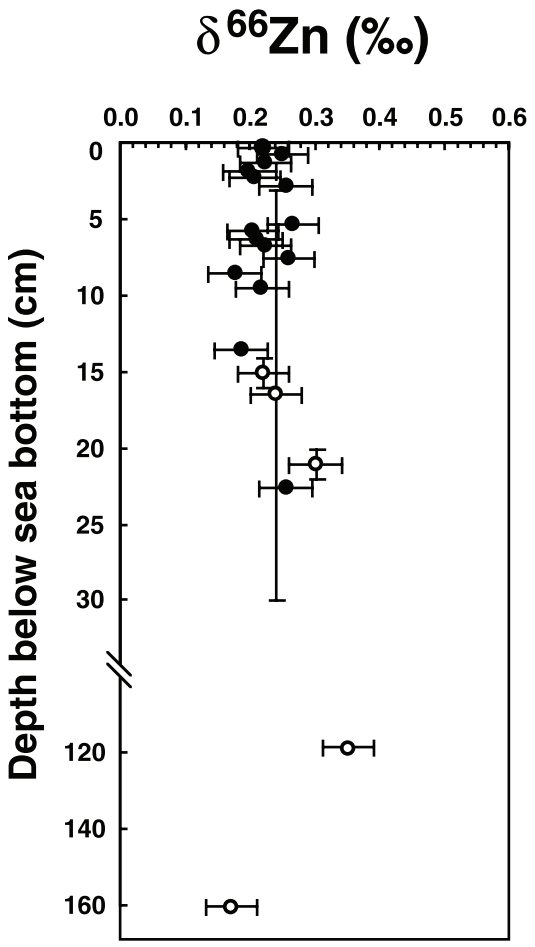

Figure 7. Figure 7. Distribution of δ^{66}Zn in sediments as a function of depth below bottom at the mesotrophic site of EUMELI (KTB 14), central Atlantic (solid circles), and from RC 17-203, central Pacific (open circles).

properties is distorted by the long time covered even by the smallest samples. It is, nevertheless, clear that the higher values of δ^{66}Zn in ferromanganese nodules are preferentially associated with temperate and subpolar latitudes, with the Circum-Antarctic Current, and with the Bengala upwelling (Figure 2). Higher values of biological productivity are common at high latitudes and in coastal upwelling areas (Figure 2) but are also observed in equatorial regions. The highest δ^{66}Zn value of all the sediments is indeed observed in the TT013 19MC carbonate ooze collected in the equatorial Pacific, where productivity is strong. We feel, however, that the local strength of the primary productivity has a rather complicated zonal distribution and is therefore unlikely to control the Zn isotopic composition of the ocean. In contrast, the difference between summer and winter productivity shows a fairly strong zonal contrast that varies rather smoothly with the latitude. In Figure 9 we contoured the modulus of the difference between the January and June productivity values from the data published by *Antoine et al*. [1996]. The amplitude of this variation is weaker at low latitude because equatorial surface waters are replenished by deep water essentially at the same rate all year round, whereas anticyclonic circulation keeps tropical surface waters essentially barren. In contrast, the seasonal variation is stronger at temperate and subpolar latitudes. It can be conjectured (Figure 10) that at higher latitudes, biological activity during the spring removes nutrients from surface waters and therefore preferentially depletes the lighter isotopes of most elements. By a mechanism similar to that observed at EUMELI but probably exaggerated by the latitude, stable seasonal thermocline prevents replenishment by deeper water until the next fall, and therefore isotopic fractionation becomes very significant, in contrast with equatorial areas where upwelling breaks through the depleted surface waters. In this respect, the pattern of Zn isotopic biochemical fractionation in the water column would be very similar to that recently identified in the Southern Ocean by *Sigman et al*. [1999] for nitrogen isotopes in dissolved nitrates. The value of the δ^{66}Zn signal with respect to that of δ^{15}N would be its presumably better preservation in the sedimentary record.

[25] The present interpretation is strengthened by the absence of prominent contrast between the Zn isotope composition of different oceans, at least as far as nodule isotopic patterns reflect those of seawater. If local productivity and remineralization were the only mechanisms that account for Zn isotopic variations in seawater and, presumably, for the geographic distribution of δ^{66}Zn in ferromanganese nodules, a relationship with the mean age of seawater in each basin should be observed. Within the extent to which the present data on solid material reflect seawater properties, we therefore ascribe the isotopic fluctuations to the seasonal variation of primary productivity. Because of the relatively close similarity of Zn and Cd overall chemistry, we suggest that the understanding of the apparent discrepancy between the glacial/interglacial changes in productivity indicated by carbon isotopes and the Cd content of foraminifera in core samples taken from the Circum-Antarctic Current [*Boyle and Keigwin*, 1985/1986; *Boyle*, 1992] may benefit from Zn isotopic studies in Quaternary sediments.

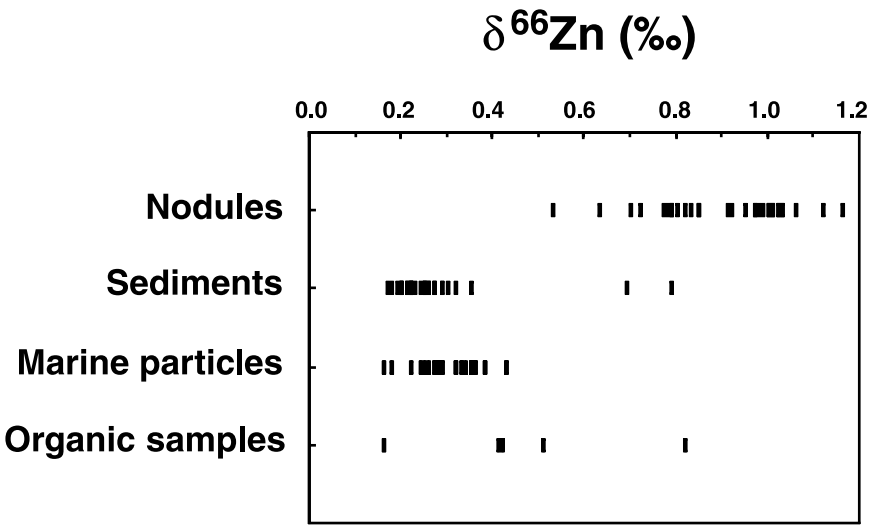

Figure 8. Summary of δ^{66}Zn in nodules, sediments, marine particles, and organic samples. The analytical error is ±0.04‰.

[26] It is not possible at this stage to assess the range of isotopic compositions for Zn dissolved in seawater. From the previous discussion on preferential uptake of ^{64}Zn by organic material we may infer that the seawater δ^{66}Zn values are higher than those obtained on organic material (0.42–0.82‰). It is, however, possible to take advantage of the fact that equilibrium fractionation of Zn isotopes between mineral phases and seawater is likely to be small. Weathering does not seem to affect the δ^{66}Zn to a large extent: the sediments with the largest lithogenic fraction and loess are isotopically indistinguishable from the mantle as represented by the Réunion Island basalt. It may therefore be

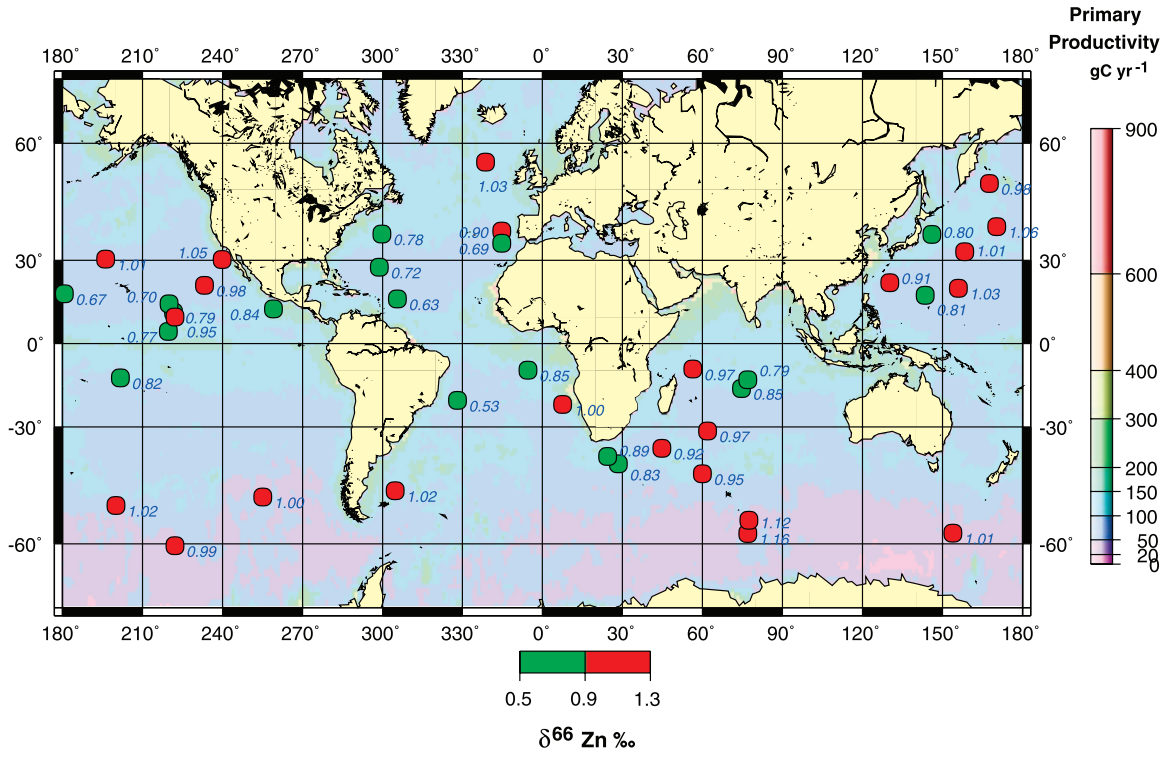

Figure 9. Distribution of δ^{66}Zn (‰) values in ferromanganese nodules with respect to the modulus of the difference between summer and winter productivity. Productivity data are from *Antoine et al.* [1996].

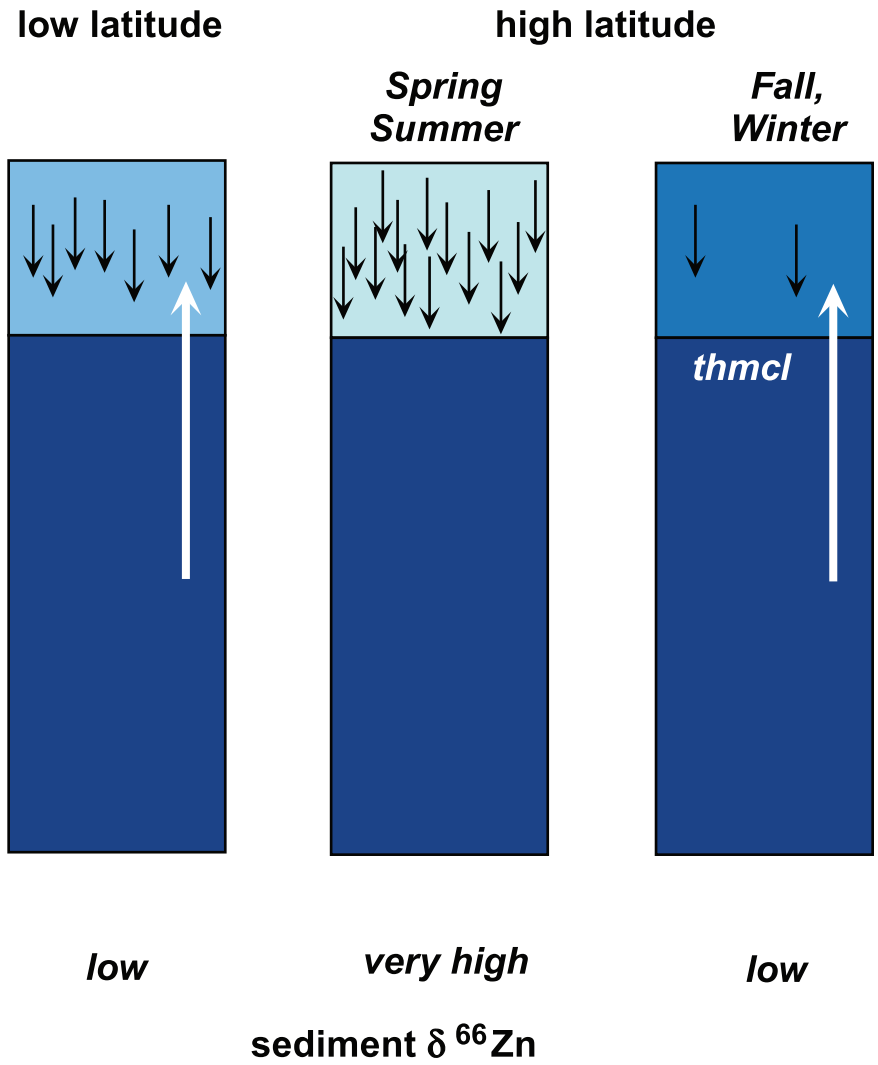

Figure 10. Sketch of the contrast in sediments δ^{66}Zn resulting from steady state replenishment of surface water at low latitude and seasonal replenishment at high latitude. On the right, exhaustion of the light isotope ^{64}Zn reasults from the presence of a stable seasonal thermocline (thmcl) during the high-productivity season. The downpointing arrows represent biogenic particle sedimentation.

argued that the δ^{66}Zn of ferromanganese nodules and seawater are very similar. The fractionation of carbon and oxygen isotopes between seawater and carbonates normally takes place at near equilibrium. We anticipate a similar behavior for ^{66}Zn/^{64}Zn equilibrium fractionation, which, because of the small mass difference, may hardly be observable. As discussed above, the difference between the δ^{66}Zn values of the NBP6904 3MC2 siliceous sediment (0.69‰) and of the ferromanganese nodules (1.0‰) from the same area of the South Pacific is probably due to the presence of a low δ^{66}Zn lithogenic component in the siliceous ooze, in which the Zn inventory should otherwise be dominated by ferromanganese coatings. It represents a probable maximum value for the fractionation between silicates and oxihydroxides and therefore between silicates and seawater. If the δ^{66}Zn values in carbonates actually reflect the ambient seawater values, the potential of Zn isotopic compositions for tracing the amplitude of seasonal productivity fluctuations in ancient oceans through carbonate analysis becomes quite appealing. At this point of technical development, however, the Zn content of carbonates (a few tens to a few hundreds of ppm [*Boyle*, 1981]) does not allow the isotopic composition of isolated foraminifera to be analyzed.

[27] With a range of δ^{66}Zn of 0.24 ± 0.14‰ (2-σ), the Zn from the particles at the EUMELI site resembles that of typical detrital samples, which seems inconsistent with the distribution of the

lithogenic, carbonate, and organic fractions in the sediment trap material. We consider that this agreement is largely fortuitous. In spite of the lack of data documenting the δ^{66}Zn of individual fractions, it is likely that the lighter organic fraction and the heavier carbonate fraction balance each other so that the bulk material happens to reproduce a value typical of clay-dominated sediment.

6. Conclusion

[28] These new measurements of Zn isotopic compositions in marine samples show that there is significant variation between nodules, particles, and sediments. There is no evidence of a relationship with aging of the deep water masses. In contrast, the isotopic signal of Zn may trace the strength of seasonal variations of the biological productivity and particulate remineralization. In which case Zn isotopes have a strong potential in oceanography and paleoceanography. Complementary measurements and laboratory experiments are now required to assess the existence of chemical and/or biological fractionation process of Zn isotopes.

Acknowledgments

[29] We are grateful to N. Leblond for the EUMELI samples (French JGOFS). We specially thank C. Jeandel and B. Hamelin for advice. We thank R. Anderson, R. Lotti, J.-L. Reyss, F. Simien, and M. Fontugne for sediment samples; J. Vervoort and W. Abouchami for nodules samples; F. Grousset for the sample of eolian dust; J.-L. Joron for the basalt; C. Jeandel and M. Roy-Barman for CRM material; and A. Quiquerez for her blood leftovers. D. Antoine kindly made available his files on the color of the sea. We thank J.-C. Marty for helpful discussion. We would like to express our gratitude to the institutions that contributed to nodules samples set: Lamont-Doherty Earth Observatory, the Muséum d'Histoire Naturelle de Paris, and the Antarctic Core Repository. Thanks to *Wessel and Smith* [1991] for the GMT software package. We thank E. Boyle, P. van Calsteren, and an anymous reviewer for thoughtful comments on the manuscript.

References

Abouchami, W., and S. L. Goldstein (1995), A lead isotopic study of Circum-Antarctic manganese nodules, *Geochim. Cosmochim. Acta*, *59*, 1809–1820.

Abouchami, W., S. J. G. Galer, and A. Koschinsky (1999), Pb and Nd isotopes in NE Atlantic Fe-Mn crusts: Proxies for trace metal paleosources and paleocean circulation, *Geochim. Cosmochim. Acta*, *63*, 1489–1505.

Albarède, F., S. L. Goldstein, and D. Dautel (1997), The neodymium isotopic composition of manganese nodules from the Southern and Indian Oceans, the global oceanic neodymium budget, and their bearing on deep ocean circulation, *Geochim. Cosmochim. Acta*, *61*, 1277–1291.

Albarède, F., A. Simonetti, J. D. Vervoot, J. Blichert-Toft, and W. Abouchami (1998), A Hf-Nd isotopic correlation in ferromanganese nodules, *Geophys. Res. Lett.*, *25*, 3895–3898.

Antoine, D., J. M. André, and A. Morel (1996), Oceanic primary production, II, Estimation at global scale from satellite (Coastal Zone Color Scanner) chlorophyll, *Global Biogeochem. Cycles*, *10*, 57–69.

Auffret, G.-A., et al. (1992), Caractérisation sédimentologique et biologique préliminaire des sites du projet EUMELI, *C. R. Acad. Sci., Ser. II*, *314*, 187–194.

Bory, A. (1997), Etude des flux de matériel terrigène dans la colonne d'eau de l'Atlantique subtropical nord-est—Relations avec les apports atmosphériques, thèse, 265 pp., Univ. Paris VII, Paris.

Boyle, E. A. (1981), Cadmium, zinc, copper, and barium in foraminifera tests, *Earth Planet. Sci. Lett.*, *53*, 11–35.

Boyle, E. A. (1992), Cadmium and δ^{13}C paleochemical ocean distributions during the stage 2 glacial maximum, *Annu. Rev. Earth Planet. Sci.*, *20*, 245–287.

Boyle, E. A., and L. D. Keigwin (1986), Comparison of Atlantic and Pacific paleaochemical record for the last 250 000 years: Changes in deep ocean circulation and chemical inventories, *Earth Planet. Sci. Lett.*, *76*, 135–150.

Bruland, K. W. (1980), Oceanographic distributions of cadmium, zinc, nickel and copper in the North Pacific, *Earth Planet. Sci. Lett.*, *47*, 176–198.

Bruland, K. W., and R. P. Franks (1983), Mn, Ni, Cu, Zn, and Cd in the western North Atlantic, in *Trace Metals in Seawater*, NATO Conf. Ser., 4. Mar. Sci., vol. 9, pp. 395–414, Plenum, New York.

Bruland, K. W., K. J. Orians, and J. P. Cowen (1994), Reactive trace metals in the stratified central North Pacific, *Geochim. Cosmochim. Acta*, *58*, 3171–3182.

Frausto da Silva, J. J. R., and R. J. P. Williams (1991), *The Biological Chemistry of the Elements, The Inorganic Chemistry of Life*, 206 pp., Clarendon, Oxford, England.

Gawinowski, G., J. L. Birck, and C. J. Allègre (1989), Zinc isotopic composition in meteorites (abstract), *Meteoritics*, *24*, 269.

Halbach, P., M. Segl, D. Puteanus, and A. Mangini (1983), Co-fluxes and growth rates in ferromanganese deposits from central Pacific seamount areas, *Nature*, *304*, 716–719.

Jickells, T. D., P. P. Newton, P. King, R. S. Lampitt, and C. Boutle (1996), A comparison of sediment trap records of particle fluxes from 19 to 48°N in the northeast Atlantic and their relation to surface water productivity, *Deep Sea Res., Part I*, *43*, 971–986.

Leblond, N., E. Nicolas, and J.-C. Marty (1995), Rapport d'activité de la cellule ''Traitement pieges'', Eutrophic, Mesotrophic, and Oligotrophic Sites, Joint Global Flux Study, Villefranche-sur-Mer, France.

Legeleux, F., J.-L. Reyss, and S. Schmidt (1994), Particle mixing rates in sediments of the northeast tropical Atlantic: Evidence from $^{210}Pb_{XS}$, ^{137}Cs, $^{228}Th_{XS}$ and $^{234}Th_{XS}$ down core distributions, *Earth Planet. Sci. Lett.*, *128*, 545–562.

Lippard, S. J., and J. M. Berg (1994), *Principles of Bioinorganic Chemistry*, 411 pp., Univ. Sci. Books, Mill Valley, Calif.

Loss, R. D., and G. W. Lugmair (1989), On the distribution of zinc isotope anomalies within Allende CAIs (abstract), *Meteoritics*, *24*, 295.

Loss, R. D., and G. W. Lugmair (1990), Zinc isotope anomalies in Allende meteorite inclusions, *Astrophys. J.*, *360*, L59–L62.

Maréchal, C. N. (1998), Géochimie isotopique du cuivre et du zinc: Méthode, variabilité naturelle et application océa-

nographique, thèse, 260 pp., Univ. J. Fourier Grenoble I, Grenoble, France.

Maréchal, C. N., P. Télouk, and F. Albarède (1999), Precise analysis of copper and zinc isotopic compositions by plasma-source mass spectrometry, *Chem. Geol.*, *156*, 251–273.

Martin, J. H., and S. E. Fitzwater (1988), Iron deficiency limits phytoplankton growth in the north-east Pacific subarctic, *Nature*, *331*, 341–343.

Morel, A. (1996), An ocean flux study in eutrophic, mesotrophic and oligotrophic situations: The EUMELI program, *Deep Sea Res., Part I*, *43*, 1185–1190.

Morel, F. M. M., R. J. M. Hudson, and N. M. Price (1991), Limitation of productivity by trace metals in the sea, *Limnol. Oceanogr.*, *36*, 1742–1755.

Rosman, K. J. R. (1972), A survey of the isotopic and elemental abundances of zinc, *Geochim. Cosmochim. Acta*, *36*, 801–819.

Saager, P. M. (1994), On the relationships between dissolved trace metals and nutrients in seawater, thèse, 240 pp., Univ. Vrije, Amsterdam.

Sigman, D. M., M. A. Altabet, D. C. McCorkle, R. Francois, and G. Fisher (1999), The δ^{15}N of nitrate in the Southern Ocean: Consumption of nitrate in surface waters, *Global Geochem. Cycles*, *13*, 1149–1166.

Völkening, J., and D. A. Papanastassiou (1990), Zinc isotope anomalies, *Astrophys. J.*, *358*, L29–L32.

Wefer, G., and G. Fischer (1993), Seasonal patterns of vertical particle flux in equatorial and coastal upwelling areas of the eastern Atlantic, *Deep Sea Res.*, *40*, 1613–1645.

Wessel, P., and W. H. F. Smith (1991), Free software helps map and display data, *Eos Trans AGU*, *72*, 441, 445–446.